

Microstructure Study of Ordinary Concrete Containing High Grade Portland Cement

Mohammadhossein Mansourghanaei^{1,*}

Received: 2025/04/19

Accepted: 2025/07/29

Abstract

In this experimental study, a mixture design of ordinary concrete containing Portland cement (OPCC) with a grade of 500 kg/m³ was made and compressive strength tests were performed at 7, 28 and 90 days of curing, and X-ray diffraction spectrometer (XRD) and scanning electron microscopy (SEM) imaging were performed on concrete samples at 90 days of curing at 21 °C to evaluate the microstructure of the concrete and to compare it with the test results of this study. Increasing the curing age due to the progress of the polymerization process (hydration) improved the results of the concrete compressive strength test. In this regard, at 90 days of curing, a compressive strength of 64.92 MPa was obtained, which was an increase of 79.48% compared to 7 days. SEM and XRD results indicate that a large part of the polymerization process has been completed and a high volume of hydrated calcium aluminosilicate gel called ettringite gel (C-A-S-H) and hydrated calcium silicate gel called tobermorite gel (C-S-H) has been produced in the concrete mix. The reduction in the amount of calcium hydroxide (Ca(OH)₂) crystals in the XRD results indicates that this product has a good contribution to the hydration process and the production of hydrated gels. The high grade of cement used has played a significant role in increasing the volume of C-S-H gel production (as the main product of the chemical reaction process in OPCC) and filling the pores, cracks and capillary pores in the microstructure matrix of OPCC.

Keywords: OPCC, C-S-H, XRD, SEM, Concrete Microstructure

* Corresponding Author. E-mail: Mhm.Ghanaei@Gmail.Com

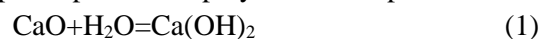
¹ Ph.D. in Civil Engineering, Department of Civil Engineering, Chalous Branch, Islamic Azad University, Chalous, Iran

1. Introduction

One of the methods for improving the mechanical properties and durability of OPCC is to increase the cement content in the mix design of this type of concrete. Research has shown that by increasing the cement content in concrete and keeping the water-cement ratio low, the mechanical properties and durability of concrete can be increased, and the poor performance of concrete in these conditions can be compensated by adding a superplasticizer [1-7]. In the meantime, controlling the water-cement ratio is of particular importance for improving properties. In this regard, research by Khaloui et al. showed that increasing the cement content at the same water-cement ratio causes a decrease in the results of the compressive strength test at the age of 7 days of curing, but has no effect on the compressive strength at the age of 90 days of curing [8]. In concretes with a low water-to-cement ratio, the high amount of cement consumption causes a higher concentration of the cement paste and a decrease in the space for available water. As a result of the cement particles coming closer together, after the polymerization process (hydration or polymerization), the pores of the concrete become smaller, and as the polymerization reaction continues, these small pores are also blocked [9].

Concrete is structurally divided into two parts: microstructure and macrostructure. The macrostructure of concrete often consists of aggregates and hydrated cement paste, which can be seen with the naked eye, but the microstructure of concrete, which often consists of pores, cracks, interlayer capillary pores, hydrated gels and other non-hydrated particles smaller than micrometers, can only be seen with an electron microscope. Any changes in the mechanical, rheological and durability properties of hardened concrete begin with the microstructure of concrete. As a result, understanding this part of concrete is of great help in interpreting the results of tests to

determine the mechanical, rheological and durability properties of concrete. Cementitious materials, along with moisture (water, alkaline solutions, etc.), produce hydrated pastes (gels) by creating a chemical reaction and carrying out the polymerization process. The most common adhesive gels used in the construction industry are produced from Portland cement, a material that dates back two hundred years [10]. In this regard, in OPCC, the combination of calcium oxide, silica oxide in varying proportions with water leads to the production of a C-S-H. This gel, with a variable and amorphous structure, constitutes a large part (according to Mehta and Monteiro [11,12], 50-60%) of the volume of the cement paste. It is the main reason for the creation of mechanical properties and durability in concrete [13,14]. According to equation 1, the combination of calcium oxide with water leads to the production of calcium hydroxide crystals called portlandite (Ca(OH)_2), which occupies the second place in the volume of cement paste (according to Mehta and Monteiro [11] 20 to 25 percent), this compound is the main factor activating the chemical reaction in the polymerization process. The combination of sulfate, aluminum and calcium oxides with water leads to the production of C-A-S-H, which occupies the third place in the volume of cement paste (according to Mehta and Monteiro [11] 15 to 20 percent). The remaining volume of hydrated cement paste belongs to unhydrated clinker grains and other components that did not participate in the polymerization process.



In concretes in which the hydration process of cement particles is well carried out, the volume of C-S-H gel is at its highest value and in this regard, as the polymerization process progresses, the volume of Ca(OH)_2 and other gels is reduced. The lesser effect of Ca(OH)_2 in improving the strength of the hardened cement paste structure is due to van der Waals forces (intermolecular attraction force) and its large particle size. The degree of adhesion depends on the development and nature of the particle

Microstructure Study of Ordinary Concrete Containing High Grade Portland Cement

surface, small crystals of C-S-H and C-A-S-H and hexagonal hydrated calcium aluminate which have a large lateral surface provide this adhesion. The presence of $\text{Ca}(\text{OH})_2$ and C-A-S-H crystals in concrete weakens it against attack by acids and sulfates. The chemical reaction mechanism in the microstructure of OPCC is as follows: initially, according to equation 1, $\text{Ca}(\text{OH})_2$ is formed in the mixture, this substance causes the dissolution of other adhesive materials in the mixture, and then the nucleation of sulfate and silica complexes begins. After the cement particles are dissolved, the nucleation of hydrated gels begins and the complexes penetrate into the gel phase and help develop the polymerization process. C-S-H gel is known as the main product of this mechanism, which plays a major role in the strength of hardened concrete. This gel has a variable chemical formula. The size of the C-S-H gel structure in OPCC has been estimated to be in the range of 1.4 nm (14 angstroms) [14]. The first direct-based model for C-S-H gel was proposed in 1952 by Bernal and his colleagues [15]. Figure 1 shows a diagram of the direct model for C-S-H gel, where P is represented as a silicate tetrahedron at the O-O edges connected to the central Ca-O layer (paired tetrahedron) and the unconnected crystals are known as B (bridged tetrahedron) [14]. Studying the atomic structure of C-S-H has always been a challenge due to its disorder and compositional variance [16-18]. However, Pelling et al. [19] presented an atomic modeling method for the molecular structure of C-S-H, which they proposed to use to study elastic deformations and cracks in the structure of this gel. Numerous studies have been conducted on the mechanical properties and crack growth mechanisms of C-S-H. In this regard, the investigation of the crack development mechanism and mechanical properties of this gel using the Clay FF force field has been presented by Hu et al. [20,21] and the effect of the percentage of water on the mechanical properties of C-S-H gel has been presented by

Shahsavari et al. [22]. According to these studies, in hydrated cements with calcium to silica (Ca/Si) ratios in the range of 1.67, the indentation modulus of C-S-H gel under CSH-FF force has been shown to be between 60 and 70 MPa, and under these conditions, the effect of hydroxyl groups on the structure is partially ignored. Bauchi et al. [23] used the Reax FF force field to investigate the toughness of the C-S-H gel structure. Palkovic et al. [24] also investigated the effect of combined loads on the C-S-H gel structure. Lin et al. [25] also investigated the dynamic mechanical properties of C-S-H gel structures under seismic compressive loads. Research has shown that reducing the calcium to silica (Ca/Si) ratio in cement leads to morphological changes in the C-S-H structure and produces a final product with high density and low porosity [17]. In this experimental study, the investigation of the microstructural properties of high-grade OPCC (500 kg/m^3) made of Portland cement is proposed as an innovative design, considering the compressive strength test and XRD and SEM analysis, and considering the high microstructural and strength properties of this type of concrete, it can be used for structural applications requiring high mechanical properties and durability.

The innovations in this research are as follows:

- 1- The use of high cement grade in OPCC leads to improved concrete microstructure and, as a result, superior mechanical properties and durability in concrete.
- 2- The effect of increasing the cement grade in OPCC on the microstructure of concrete was investigated, which showed superior results compared to concrete with a lower grade and Portland cement consumption.
- 3- XRD analysis was conducted on OPCC with a high cement content, which showed superior results compared to concrete with a lower content of Portland cement.

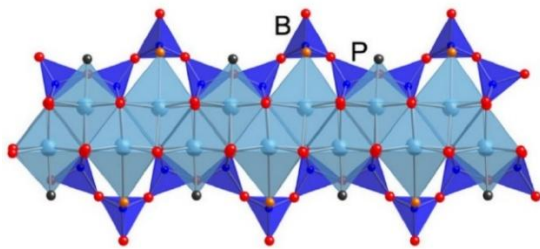


Figure 1. Structure of C-S-H Gel

2. Materials

In this experimental study, the cement used with a specific gravity of 3250 kg/m³ and a specific surface area of 3100 cm²/g is Portland Type 2, produced by the Gilan Sabz Cement Industries Factory (Dilman), which is produced under the En 197-1 standard. Table 1 shows the chemical characteristics of the cement used. The water used to prepare lime water and make the mixture design in the current study is from the drinking water of Lahijan city. This water has a pH in the range of 5.6 to 5.7 and a specific gravity of 1000 kg/m³. According to Section 2-4-10-9 and 3-4-10-9 of the fourth edition of the National Building Regulations of Iran, water that is drinkable, has no distinct taste or odor, and is clean and clear can be used in concrete without testing, unless previous records indicate that this water is unsuitable for concrete. The aggregate grading curve used is within the ASTM C33 standard range as shown in Figure 2. The materials used from Lahijan sand and gravel factories were prepared according to ASTM C33 standards and purified to remove organic impurities. Some properties of fine and coarse aggregates were determined based on Table 2. The superplasticizer used was a fourth-generation normal polycarboxylate-based product from Durocem Middle East Company under the trade name Flowcem R700. This material was used to compensate for the poor performance and maintain the fluidity of the mortar mixture [1-6] due to the high grade of Portland cement used in concrete. Some of the characteristics of the polycarboxylate normal superplasticizer (PCNS) are presented in Table 3.

Table 1. Chemical Characteristics of Portland cement

| Component | % |
|--------------------------------|------|
| SiO ₂ | 21.3 |
| Al ₂ O ₃ | 4.7 |
| Fe ₂ O ₃ | 4.3 |
| CaO | 62.7 |
| MgO | 2.1 |
| SO ₃ | 2 |
| K ₂ O | 0.65 |
| Na ₂ O | 0.18 |
| LOI | 1.84 |
| TiO ₂ | - |

Table 2. Aggregate Specifications

| Concrete Aggregates | Gravel | Sand |
|------------------------------|-----------|---------|
| Minimum Diameter | 4.75 (mm) | 75 (μm) |
| Maximum Diameter (mm) | 19 | 4.75 |
| Modulus of Elasticity (mm) | 5.7 | 2.85 |
| Density (kg/m ³) | 2750 | 2650 |
| Water Absorption (%) | 2.2 | 2.9 |

Table 3. PCNS Specifications

| Chemical Formula | Normal Polycarboxylate |
|------------------------------|------------------------|
| Physical Condition | Liquid |
| Color | Light Brown |
| Density (kg/m ³) | 1100 |
| Consumption Standard | ASTM C494 |
| pH | 7 |

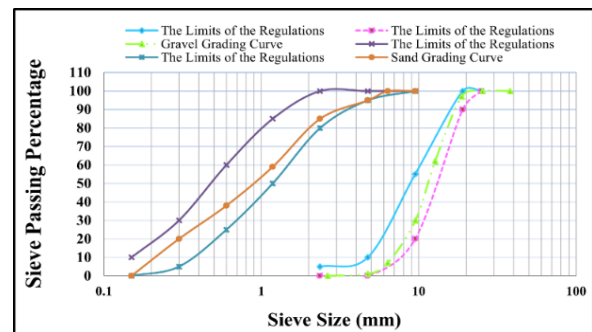


Figure 2. Aggregate Curve

3. Mix Design Sample Preparation and Curing

A typical concrete mix plan was prepared based on the proposal of the American Concrete Association under the recommendation of the ACI 211.1-89 committee based on Table 4. In this regard, the specific gravity of the concrete was determined to be 2397.9 kg/m³ and the water-to-cement ratio was determined to be 0.45. First, dry materials were poured into the

Microstructure Study of Ordinary Concrete Containing High Grade Portland Cement

rotating mixer and the process of mixing the concrete components lasted for 1.5 minutes, then water and superplasticizer were added to the mixture and the mixing of the materials lasted for another 2 minutes. Next, the concrete molds that had been previously foiled and lubricated were filled with concrete in three

stages, and in each stage, 25 blows were given to the concrete with a special rod to compact the concrete components. The samples were stored for 24 hours at a temperature of 21 °C in a dry environment and, after demolding, they were stored and cured in lime water at a temperature of 21 °C until the test time.

Table 4. Concrete Mix Design Specifications

| | Consumable Materials | | | | |
|---------------------------------------|----------------------|--------|--------|--------|--------|
| | Water | Cement | Gravel | Sand | PCNS |
| Specific Gravity (kg/m ³) | 1000 | 3250 | 2750 | 2650 | 1100 |
| Consumption Weight (kg) | 225 | 500 | 1000 | 666.15 | 6.75 |
| Consumption Weight (%) | 9.38 | 20.85 | 41.7 | 27.78 | 0.0028 |

4. Standards and Test Method

The compressive strength test of concrete at the age of 7, 28 and 90 days was carried out in accordance with the BS 12390-3 standard on cubic samples with dimensions of 10×10×10 cm. In this regard, the samples were placed in a concrete jack machine in such a way that the two opposite surfaces that were adjacent to the mold during concrete pouring were in contact with the upper and lower stirrups of the machine. After the samples were solidified, the force loading was carried out within the standard range at a speed of 0.9 MPa/s (54 MPa/min) in a constant, uniform manner, without sudden changes and perpendicular to the direction of concreting until the moment of concrete sample failure. The maximum applied load determines the resistance of the concrete sample to the applied compressive force. XRD analysis was carried out at the age of 90 days using an XRD with the Philips PW1730 model. In this regard, crushed samples taken from the center of the concrete sample were placed inside the device and during the test, a diffraction diagram of concrete crystals was prepared. The data obtained from XRD is in the form of photon intensity in terms of detector angle 2θ, which is presented as a list of peak locations and their intensities on the graphs. SEM image analysis was performed at a curing age of 90 days using a SEM with the FEI Quanta200 model. In this regard, the crushed concrete

sample was placed in the device and images were recorded at a scale of 3 and 20 μm and then subjected to microstructural examination.

5. Test Results and Interpretation of Results

5.1. Compressive Strength Test Results

The results of the concrete compressive strength test are shown in the graph of Figure 3. Research has shown that the compressive strength of concrete increases rapidly at early ages [26-29]. Based on the results of this study, it is observed that increasing the curing age of concrete has improved the results. These results have also been obtained in the research of others [1,2]. This is mainly due to the progress of the polymerization process in the microstructure of concrete, which has led to the production of a high volume of C-A-S-H and C-S-H gels in the hydrated cement paste. These gels, by filling the pores, pores, cracks, microcracks and creating connections and bonds in the interfacial transition zones (ITZ) at the interface between the aggregate and the cement paste, also by filling the interlayer capillary pores, create strength in hardened concrete [3,4]. Research by Kamasi et al. shows that increasing hydrated gels in concrete composition has a favorable effect on improving the results of compressive strength test [30]. In this paper, the lowest (43.63 MPa) and highest (64.92 MPa)

compressive strength acquisition rate at 7 and 90 days curing age, respectively, is accompanied by an improvement of 79.48% (90 vs. 7 days). The results of XRD and SEM analysis in this study confirm the amount and volume of chemical activity of cementitious materials in the polymerization process, which has led to improved results of compressive strength test.

Similar research on OPCC cured in lime water [4,5] shows that increasing the curing age of concrete leads to improved compressive strength in this type of concrete [1,2], and similar results were obtained in other research using cement and aggregate with the characteristics of the cement and aggregate used in this study [3].

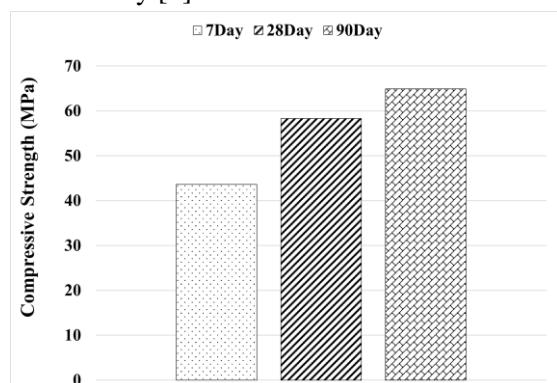


Figure 3. Compressive Strength Test Results

5.2. XRD Analysis Results

In the present study, the results of XRD analysis on concrete samples in this study are shown in Figure 4. Based on these results, it is observed that most of the large peaks in the graph occurred in the regions of 16 to 29 and also 60 degrees, which is due to the arrangement and atomic structure of the concrete sample. By examining the angle of formation of the peaks and their relative intensity, the type of materials and peak phases present in the graph obtained from XRD can be identified. Aluminum phosphate compounds with a maximum peak height of 2670 at an angle of 59.85 degrees, followed by calcium hydroxide with a maximum peak height of 2452 at an angle of 24.41 degrees, titanium oxide with a maximum

peak height of 1794 at an angle of 24.29 degrees, calcite with a maximum peak height of 1600 at an angle of 26.45 degrees, and dolomite with a maximum peak height of 671 at an angle of 17.92 degrees, have the highest dispersion. Ca(OH)_2 is the result of the combination of calcium oxide and water and is known as a reactive compound for other cementitious materials in the polymerization process. The presence of this compound in the second rank of elements with the highest dispersion is due to the incomplete polymerization process, of course, with increasing curing age in concrete and in the long term, with greater participation of Ca(OH)_2 in the chemical process, the volume of this material in the concrete composition will be reduced. The high grade of Portland cement in concrete increases the speed of the polymerization process, as a result, some cementitious materials will not have the opportunity to participate in the chemical process, this is also one of the factors that increase the volume of Ca(OH)_2 in the XRD of the concrete composition [3,4].

Similar research on OPCC cured in lime water [4,5] shows that the results of X-ray diffraction (XRD) analysis in the height of the peaks obtained for each of the main components such as aluminum phosphate, calcium hydroxide, titanium oxide, calcite and dolomite are very close to the concrete obtained in the present study [1,2].

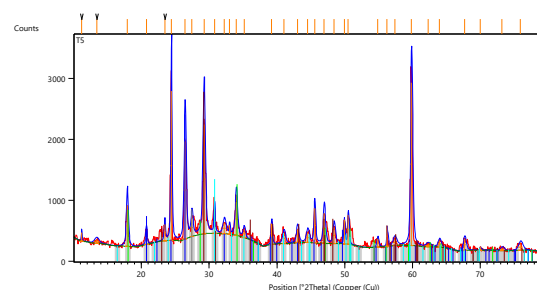


Figure 4. XRD Result

5.3. SEM Analysis Results

SEM analysis for images at 3 and 20 μm scales obtained from concrete samples at a curing age of 90 days and a temperature of 21 °C in this

Microstructure Study of Ordinary Concrete Containing High Grade Portland Cement

study is shown in Figure 5. The results obtained from the electron microscope can be of great help in diagnosing the microstructure and behavior of concrete. According to the images obtained from SEM, it is observed that the microstructure of concrete consists of three basic and distinct phases as follows [1-5]:

1- The first phase includes polymerization products containing C-A-S-H and C-S-H gels, which are mainly dark in SEM images. According to the studies conducted, the volume of C-S-H gel is at its highest.

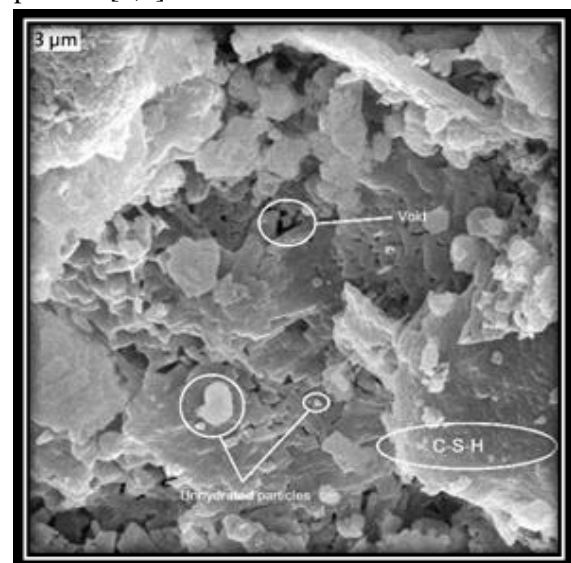
2- The second phase includes unreacted crystals, which are a result of impurities in the raw materials or unreacted particles in the polymerization process, and are mainly white in SEM images.

3- The third phase includes the way cement paste bonds with aggregates in the ITZ.

Microstructural images indicate that the volume of hydrated gels such as C-A-S-H and C-S-H are produced in appropriate amounts in the mixture. Unhydrated particles in the mixture can be caused by $\text{Ca}(\text{OH})_2$ or other cement particles that have not been able to participate in the chemical reaction process. In this regard, large unhydrated particles (white dots) are often related to $\text{Ca}(\text{OH})_2$ and finer particles are unhydrated clinker grains. The presence of pores and tree structure that indicate the weakness of the mixture are rarely seen in the mixture and this can be due to the high grade of cement used in the concrete mix design. Research has shown that in the bulk part of Portland cement paste, ions such as calcium, sulfate, hydroxide and aluminate, which are formed through aerobic (dissolving) into calcium silicate and calcium aluminate, combine and form C-A-S-H and $\text{Ca}(\text{OH})_2$ gels, meaning that C-A-S-H is formed as a result of the reaction of calcium aluminate with calcium sulfate, and as the polymerization stage progresses, weak C-S-H crystals and the second generation of crystals formed from $\text{Ca}(\text{OH})_2$ and C-A-S-H gel begin to fill the empty spaces in the C-A-S-H and $\text{Ca}(\text{OH})_2$ network, and with

this operation, the density, hardness and ITZ strength of concrete increase [5]. Due to the greater solubility of $\text{Ca}(\text{OH})_2$ compared to C-S-H, the excessive presence of this substance in the concrete composition has an adverse effect on the chemical durability of concrete against acids. On the other hand, the calcium aluminum sulfate (C-A-S-H) compound, which forms part of the hydrated gels in the matrix of OPCC, is vulnerable to sulfate attack. Research has shown that after the materials used in the preparation and manufacture of concrete are combined, a chemical reaction (polymerization) process begins between the cementitious materials and water. The speed and extent of the formation of the C-S-H gel, which is the main product of the polymerization process, depends mainly on the properties and proportions of the cementitious materials and water. This compound (C-S-H) has better resistance to acidic and sulfate environments than the other compounds mentioned and is the main reason for the strength of hardened concrete.

Similar research on OPCC cured in lime water [4,5] shows that in SEM images of concrete, the volume of hydrated gels produced at the corresponding curing age is at the same level, as are unhydrated $\text{Ca}(\text{OH})_2$ particles and cement particles that did not participate in the hydration process [1,3].



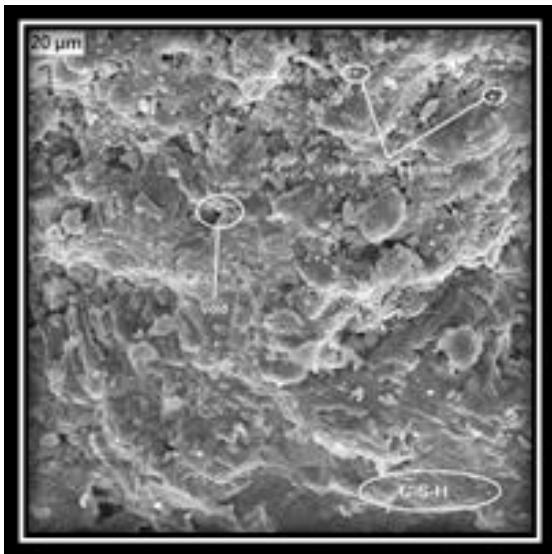


Figure 5. SEM Images

6. Conclusion

In this experimental study, the microstructure of OPCC with a grade of 500 kg/m³ at a temperature of 21 °C was evaluated. In this regard, compressive strength tests and XRD and SEM analysis were performed on concrete samples. The results of this study are presented as follows.

1- In the compressive strength test, increasing the curing age improved the results, so that at a curing age of 90 days, the maximum compressive strength was obtained at 64.92 MPa, which was an improvement of 79.48% compared to the 7-day curing age in concrete.

2- In XRD analysis, aluminum phosphate compounds with a maximum peak height of 2670 at an angle of 59.85 degrees, followed by calcium hydroxide with a maximum peak height of 2452 at an angle of 24.41 degrees, titanium oxide with a maximum peak height of 1794 at an angle of 24.29 degrees, calcite with a maximum peak height of 1600 at an angle of 26.45 degrees, and dolomite with a maximum peak height of 671 at an angle of 17.92 degrees, have the highest dispersion.

3- The presence of Ca(OH)₂ with a high peak height in the XRD is due to the incomplete polymerization process. The high cement content in the concrete composition has

exacerbated this issue by accelerating the polymerization process.

4- In the analysis of SEM images, the volume of hydrated gels is seen in high amounts in the cement matrix due to the high grade of Portland cement in the composition and completion of a large part of the polymerization process. This has led to the filling of cracks, cavities and capillary pores and has reduced their volume in the composition.

5- The evaluation of SEM images of the microstructure of the concrete was in agreement and overlap with the results of the compressive strength test and XRD analysis.

7. Abbreviations

OPCC: Ordinary Portland Cement Concrete

GPC: Geopolymer Concrete

GBFS: Granulated Blast Furnace Slag

POFs: Polyolefin Fibers

NS: Nano Silica

SEM: Scanning Electron Microscope

AAS: Active Alkali Solution

XRD: X-ray Diffraction Spectrometer

C-A-S-H: hydrated Calcium Aluminosilicate

C-S-H: Hydrated Calcium Silicate

PCNS: Polycarboxylate Normal Superplasticizer

8. Reference

– Mansourghanaei, M., Biklaryan, M., & Mardookhpour, A. (2024). Durability and mechanical properties of granulated blast furnace slag based geopolymer concrete containing polyolefin fibers and nano silica. *KSCE Journal of Civil Engineering*, 28(1), 209-219.

– Mansourghanaei, M., Biklaryan, M., & Mardookhpour, A. (2024). Experimental study of the effects of adding silica nanoparticles on the durability of geopolymer concrete. *Australian Journal of Civil Engineering*, 22(1), 81-93.

Microstructure Study of Ordinary Concrete Containing High Grade Portland Cement

- Mansourghanaei, M., Biklaryan, M., & Mardookhpour, A. (2023). Experimental study of properties of green concrete based on geopolymer materials under high temperature. *Civil Engineering Infrastructures Journal*, 56(2), 365-379.
- Mansourghanaei, M., & Mardookhpour, A. (2024). Analysis of the Numerical Results Obtained from the Experimental Examination of the Mechanical Properties of Geopolymer Concrete. *Numerical Methods in Civil Engineering*, 9(1), 31-41.
- Mansourghanaei, M., Biklaryan, M., & Mardookhpour, A. (2023). Experimental Study of Mechanical Properties of Slag Geopolymer Concrete under High Temperature, Used in Road Pavement. *International Journal of Transportation Engineering*, 11(1), 1371-1385.
- Mansourghanaei, M., & Mardookhpour, A. (2023). Investigating the Properties of Environmentally Friendly Green Concrete (Geopolymer) Under High Temperature. *Sustainable Earth Trends*, 3(4), 62-69.
- Tadaion, M., Honarmand, H., & Kalhori, M. (2010). Impact of Plasticizers on the Quality of Concrete and the Reduction of the Cement Content. *Concrete Research*, 3(2), 49-57.
- Khalooee, S., Ahmadi, B., Askarinejad, A., & Nekooei, M. (2019). The effect of cementitious materials paste volume and use of zeolite on the properties of self-compacting concrete. *Journal of Concrete Structures and Materials*, 4(1), 100-109.
- Mahmood Naderi; Rezvan Valibeigi; Seyed Mohammad Mirsafi. "Studying the Effects kind of Curing on Strengths and Permeability of Concrete". *Journal of Structural and Construction Engineering*, 5, 3, 2018, 106-123. doi: 10.22065/jsce.2017.69343.1013
- Moir, G., Cements. In *Advanced Concrete Technology: Constituent Materials*, Newman, J.; Choo, B. S., Eds. Butterworth-Heinemann: Oxford, 2003; pp 1-45.
- Mehta, P. K., & Monteiro, P. J. (2014). *Concrete: microstructure, properties, and materials*. McGraw-Hill Education.
- Lin, W., Zhang, C., Fu, J., & Xin, H. (2018). Dynamic mechanical behaviors of calcium silicate hydrate under shock compression loading using molecular dynamics simulation. *Journal of Non-Crystalline Solids*, 500, 482-486.
- Juenger, M. C. G.; Winnefeld, F.; Provis, J. L.; Ideker, J. H., *Advances in alternative cementitious binders*. *Cem. Concr. Res.* 2011, 41, 1232-1243.
- Richardson, I. G. (2008). The calcium silicate hydrates. *Cement and concrete research*, 38(2), 137-158.
- J.D. Bernal, J.W. Jeffery, H.F.W. Taylor, *Crystallographic research on the hydration of Portland cement. A first report on investigations in progress*, *Mag. Concr. Res.* 4 (11) (1952) 49–54.

- I.G. Richardson, The calcium silicate hydrates, *Cem. Concr. Res.* 38 (2008) 137–158.
- I.G. Richardson, Tobermorite/jennite- and tobermorite/calcium hydroxide-based models for the structure of C-S-H: applicability to hardened pastes of tricalcium silicate, β -dicalcium silicate, Portland cement, and blends of Portland cement with blast-furnace slag, metakaolin, or silica fume, *Cem. Concr. Res.* 34 (2004) 1733–1777.
- A.J. Allen, J.J. Thomas, H.M. Jennings, Composition and density of nanoscale calcium-silicate-hydrate in cement, *Nat. Mater.* 6 (2007) 311–316.
- R.J. Pellenq, A. Kushima, R. Shahsavari, K.J. Van Vliet, M.J. Buehler, S. Yip, F.J. Ulm, A realistic molecular model of cement hydrates, *Proc. Natl. Acad. Sci. U. S.A.* 106 (2009) 16102–16107.
- D. Hou, H. Ma, Y. Zhu, Z. Li, Calcium silicate hydrate from dry to saturated state: structure, dynamics and mechanical properties, *Acta Mater.* 67 (2014) 81–94.
- D. Hou, Y. Zhu, Y. Lu, Z. Li, Mechanical properties of calcium silicate hydrate (C-S-H) at nano-scale: a molecular dynamics study, *Mater. Chem. Phys.* 146 (2014) 503–511.
- R. Shahsavari, J.M. Pellenq, F.J. Ulm, Empirical force fields for complex hydrated calcium-silicate layered materials, *Phys. Chem. Chem. Phys.* 13 (2010) 1002–1011.
- M. Bauchy, H. Laubie, M.J.A. Qomi, C.G. Hoover, F.J. Ulm, R.J.M. Pellenq, Fracture toughness of calcium-silicate-hydrate from molecular dynamics simulations, *J. Non-Cryst. Solids* 419 (2015) 58–64.
- S.D. Palkovic, S. Yip, O. Büyüköztürk, Constitutive response of calcium-silicatehydrate layers under combined loading, *J. Am. Ceram. Soc.* 100 (2017) 713–723.
- Lin, W., Zhang, C., Fu, J., & Xin, H. (2018). Dynamic mechanical behaviors of calcium silicate hydrate under shock compression loading using molecular dynamics simulation. *Journal of Non-Crystalline Solids*, 500, 482-486.
- Abd elaty, M.a.a. (2014). Compressive strength prediction of Portland cement concrete with age using a new model. *HBRC J.* 10 (2), pp 145–155.
- Kim, J.K., Moon, Y.H., Eo, S.H. (1998). Compressive strength development of concrete with different curing time and temperature. *Cem. Concr. Res.* 28 (12), pp 1761–1773.
- Madandoust, R., Bungey, J.H., Ghayidel, R. (2012). Prediction of the concrete compressive strength by means of core testing using GMDH-type neural network and ANFIS models. *Comput. Mater. Sci.* 51 (1), pp 261–272.
- Farhad Pirmohammadi Alishah; Navid Mahmoudzadeh. "Investigation of the effect of bentonite paste index on modulus of elasticity, compressive strength and performance of

Microstructure Study of Ordinary Concrete Containing High Grade Portland Cement

plastic concrete". Civil and Project Journal, 2, 5, 2020, 87-109.

– Mehdi Komasi; shayan khosravi; hossein chobkar. "Laboratory study for optimal mixing scheme of pervious concrete containing additive of microsilica fume based on maximum compressive strength and permeability". Journal of Structural and Construction Engineering, 7, 4, 2021, 42-61. doi: 10.22065/jsce.2018.135444.1586